Trimethyl-*p*-benzoquinone Provides Excellent Structural, Spectroscopic, and Thermochemical Models for Plastoquinone-1 and Its Radical Anion

Kristopher E. Wise, Anthony K. Grafton, and Ralph A. Wheeler*

Department of Chemistry & Biochemistry, University of Oklahoma, 620 Parrington Oval, Room 208, Norman, Oklahoma 73019

Received: September 20, 1996; In Final Form: November 22, 1996[⊗]

Trimethyl-*p*-benzoquinone (TMQ) has been proposed to furnish an accurate thermochemical model for plastoquinones, key electron acceptors in oxygenic photosynthetic electron transfer. Free energy perturbation/molecular dynamics simulations combined with hybrid Hartree−Fock/density functional (HF/DF) calculations confirm that TMQ and plastoquinone-1 have approximately equal aqueous one-electron reduction potentials, within the accuracy of the calculations. HF/DF calculations using the B3LYP/6-31G(d) method also show that TMQ and its radical anion have (1) structures almost identical to those of PQ—a model for plastoquinone-1 without the isoprenoid chain's methyl groups—and its radical anion, respectively, have (2) spin densities for $TMQ^{\bullet-}$ and $PQ^{\bullet-}$ which differ by 0.01 electrons at most, and have (3) key C═O and C═C stretching frequencies for the TMQ/PQ and $TMQ^{\bullet-}/PQ^{\bullet-}$ pairs differing by only 1−8 cm^{-1}. Thus, TMQ and $TMQ^{\bullet-}$ are excellent models for the structures, spin densities, and vibrational frequencies of plastoquinones and their radical anions, respectively.

Introduction

Plastoquinone is a key intermediate in oxygenic photosynthetic electron transport.[1−4] In plant photosystem II, for example, plastoquinone-9 (PQ_9, **1a** with $n = 9$) in thylakoid membranes acts as both a primary and secondary electron acceptor and its radical anion is a secondary electron donor (see Scheme 1). A pool of plastoquinones in equilibrium with membrane-bound PQ_9 acts as a pump to carry protons across the membrane and as an electron carrier between photosystem II and the cytochrome b_6f complex.[2] Despite the biochemical importance of plastoquinones and their radical anions, only limited vibrational and spin density data are currently available and we know of no experimental structures or electron affinities. Because the measured aqueous reduction potentials for trimethyl-*p*-benzoquinone (TMQ) and plastoquinones are similar,[5,6] TMQ was proposed as a thermodynamic analog for the plastoquinones.[6] Since structural and spectroscopic data for plastoquinone are crucial as a reference for determining the effects of plastoquinone interactions with proteins, it is important to determine the suitability of TMQ and its radical anion $TMQ^{\bullet-}$ as models for the corresponding plastoquinone species. This contribution thus compares hybrid Hartree−Fock/density functional (HF/DF) calculations of the structures, vibrational frequencies, and vibrational modes of trimethyl-*p*-benzoquinone, a model for plastoquinone-1 without methyl groups on the isoprenoid side chain (PQ), and their radical anions. We also report HF/DF-derived spin densities and hyperfine coupling constants (calculated from Fermi contact spin densities)[7,8] for $TMQ^{\bullet-}$ and $PQ^{\bullet-}$ and calculated electron affinities of TMQ, PQ, and the actual plastoquinone-1 (PQ_1, including the chain-terminal methyl groups). Aqueous reduction free energies were also computed by using thermodynamic cycle/free energy perturbation calculations coupled with molecular dynamics (MD) simulations. We emphasize that this work demonstrates the similar properties of isolated and aqueous $PQ/PQ^{\bullet-}$ and $TMQ/TMQ^{\bullet-}$ species and does not address the adequacy of TMQ as a model for PQ in proteins.

Published data for PQ_9 include measured oxygen spin densities of 0.21,[9] *ab initio* MO calculations for model compounds,[10] calculated structures and hyperfine coupling constants for the radical anion of PQ_1,[11] and partial experimental IR spectra.[12,13] A C═O stretching band was experimentally observed at 1650 cm^{-1}, with a shoulder at 1635 cm^{-1}, and a C═C stretch was measured at 1620 cm^{-1}. To address the need for more information about plastoquinones and their radical anions, we present a computational study of models for the smallest plastoquinone, PQ_1 (**1a**, $n = 1$), and its reduced semiquinone radical anion (**1b**, $n = 1$, shows major resonance forms). Our primary model, chosen for computational economy, differs from PQ_1 only in the replacement of the isoprenoid chain's methyl groups by hydrogens. First, we compare calculated properties of the model plastoquinone (PQ, see Figure 1) and its radical anion ($PQ^{\bullet-}$) with those of the simpler model compound trimethyl-*p*-benzoquinone (TMQ) and its radical anion ($TMQ^{\bullet-}$) and then describe the results of thermochemical calculations to estimate electron affinities and aqueous reduction potentials. Computational methods are described in the Appendix.

Structures, Spin Properties, and Vibrational Analysis

Calculated bond distances for PQ (shown in Figure 1, along with the carbon atom numbering scheme used subsequently) and TMQ (see Figure 1) are similar to those calculated for *p*-benzoquinone[14] and show negligible differences between each other. Excluding the ring C−CH_3 and ring C−CH_2 bond distances, average differences of less than 0.001 Å for bond lengths and 0.1° for bond angles are found between the calculated structures of TMQ and PQ. For both TMQ and PQ, one C═C and both C═O bond distances are similar to those calculated for *p*-benzoquinone.[14] The C2═C3 bonds are 0.013 Å longer in TMQ and PQ, and the C−C bonds are approximately 0.03 Å longer in TMQ and PQ than in *p*-benzoquinone.

The primary structural effects of reducing PQ (Figure 1) to $PQ^{\bullet-}$ (Figure 2; Figure 2 shows atomic connectivity but does not indicate bonding) are found in the C═O, ring C═C, and

[⊗] Abstract published in *Advance ACS Abstracts,* January 15, 1997.

S1089-5639(96)02906-4 CCC: $14.00 © 1997 American Chemical Society

SCHEME 1

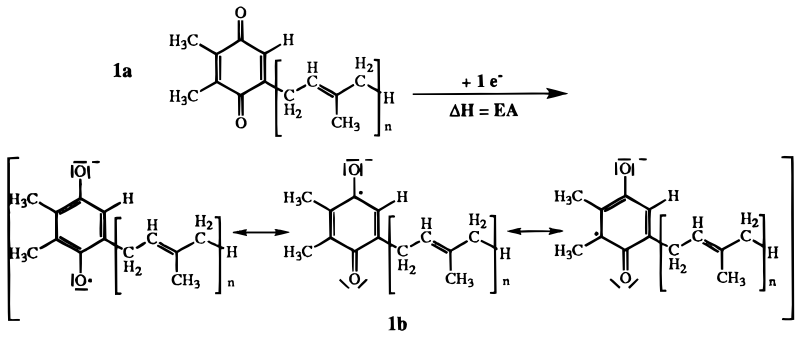

TABLE 1: B3LYP-Derived Isotropic Hyperfine Coupling Constants (in Gauss) for a Plastosemiquinone Model without Chain-Terminal Methyl Groups ($PQ^{\bullet-}$) and Trimethyl-*p*-benzosemiquinone ($TMQ^{\bullet-}$) Using Several Different Basis Sets

atom no.	$PQ^{\bullet-}$ (expt)[a]	$PQ^{\bullet-}$ 6-31G(d)	$PQ^{\bullet-}$ 6-311G(d,p)	$PQ^{\bullet-}$ [632|41]	$TMQ^{\bullet-}$ 6-31G(d)	$TMQ^{\bullet-}$ 6-311G(d,p)	$TMQ^{\bullet-}$ [632|41]
C_1		−0.95	−4.02	−3.49	−0.57	−3.72	−2.72
C_2		+2.47	−0.03	+0.69	+2.32	−0.15	+0.47
C_3		+0.75	−1.32	−0.79	+1.19	−1.11	−0.64
C_4		+1.01	−2.59	−2.13	+0.52	−2.93	−1.89
C_5		+1.49	−0.74	+0.08	+1.92	−0.46	+0.23
C_6		+2.31	−0.48	−0.05	+1.66	−0.88	−0.49
C_7		−1.43	−1.52	−1.55	−1.42	−1.53	−1.53
Av of H_7	+1.76	+2.09	+2.07	+2.13	+2.07	+2.06	+2.11
C_8		−1.09	−1.14	−1.16	−1.21	−1.26	−1.26
av of H_8	+1.90	+1.48	+1.43	+1.47	+1.67	+1.60	+1.63
C_9		−1.08	−1.24	−1.25	−1.29	−1.43	−1.44
av of H_9	+2.45	+1.01	+1.03	+1.10	+1.58	+1.58	+1.61
C_{10}		+0.44	+0.74	+0.75	n/a[b]	n/a	n/a
H_{10} proton	−0.11	−0.06	−0.07	−0.10	n/a	n/a	n/a
C_{11}		+0.04	+0.01	−0.01	n/a	n/a	n/a
av of H_{11}		+0.09	+0.09	+0.12	n/a	n/a	n/a
O_1		−8.82	−5.67	−7.54	−8.74	−5.63	−7.29
O_2		−8.83	−5.37	−7.20	−8.46	−5.42	−7.00
H_6	−2.05	−2.79	−2.49	−2.32	−2.47	−2.20	−2.10

[a] Macmillan, F.; Lendzian, F.; Renger, G.; Lubitz, W. *Biochemistry* **1995**, *34*, 245−267. [b] n/a = not available.

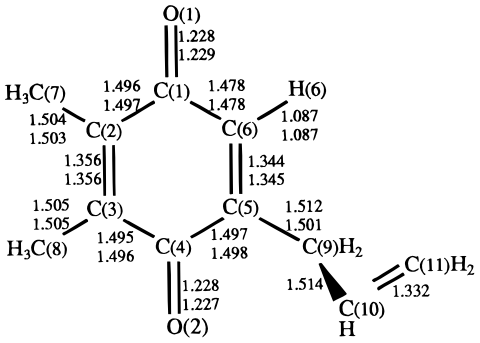

Figure 1. B3LYP/6-31G(d) calculated bond distances for PQ (upper number) and TMQ (lower number).

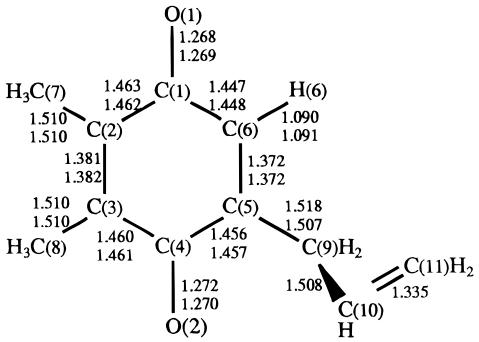

Figure 2. B3LYP/6-31G(d) calculated bond distances for $PQ^{\bullet-}$ (upper number) and $TMQ^{\bullet-}$ (lower number).

C−C bonds. The C═O and C═C bonds are each lengthened in the anion by approximately 0.04 and 0.03 Å, respectively. Conversely, the C−C single bonds are shorter in the anion by amounts ranging from 0.031 to 0.042 Å. This pattern of bond distance changes upon reducing PQ to $PQ^{\bullet-}$ and TMQ to $TMQ^{\bullet-}$ is consistent with the nodal structure of the singly occupied molecular orbital for the unsubstituted *p*-benzosemiquinone radical anion.[14−16] Finally, the geometrical differences between $PQ^{\bullet-}$ and $TMQ^{\bullet-}$ (compare bond distances in Figure 2) are similar in magnitude to the differences found between PQ and TMQ (Figure 1). Apparently, the alkyl side chain's identity has minimal impact on the quinone ring geometries of PQ, TMQ, $PQ^{\bullet-}$, and $TMQ^{\bullet-}$.

Spin densities for $PQ^{\bullet-}$ and $TMQ^{\bullet-}$, calculated by using the 6-311G(d,p) basis set, are highlighted in **2a** and **2b**, respectively, to emphasize their striking similarity. Spin densities for $TMQ^{\bullet-}$ and $PQ^{\bullet-}$ differ from each other by only 0.01, agree qualitatively with experiments for PQ_9,[9] and indicate that the first resonance form shown in **1b** is most significant. Table 1 displays isotropic hyperfine coupling constants (hfccs) for $PQ^{\bullet-}$ and $TMQ^{\bullet-}$, calculated by using three different basis sets. Hyperfine coupling constants are proportional to the spin density at a particular nucleus[7,8] and therefore give a more stringent test than spin densities of a computational method. Although all calculated proton hfccs are similar to experiment for plastoquinone radical anions,[17] qualitative differences in heavy atom hfccs calculated with the different basis sets urge caution. Since others have found that density functional methods with basis sets augmented by contracted functions in the core region give the most accurate heavy-atom hfccs,[18−20] we believe that

Chipman's basis set abbreviated [632|41][21,22] (described in the Appendix) probably yields the most accurate hfccs. Finally, we note that our calculated hfccs for $PQ^{\bullet-}$ are similar to recently published values[11] and that the calculated hfccs confirm the qualitative picture of spin density distributions shown in **2a** and **2b**.

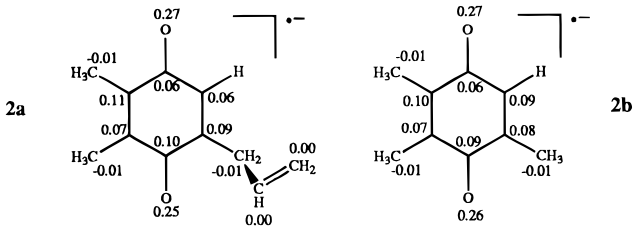

Tables 2 and 3 show the complete set of calculated vibrational frequencies and their corresponding mode descriptions for PQ, $PQ^{\bullet-}$, TMQ, and $TMQ^{\bullet-}$. Because the C═O and C═C stretching modes are most easily detectable for quinones in proteins and are used as diagnostics of quinone-protein interactions,[12] we focus on the calculated C═O and C═C modes. In general, the relative order of the PQ and TMQ modes is very similar, but the modes of TMQ appear at slightly higher frequencies. For neutral PQ, the mode at 1738 cm^{-1} is a stretching vibration mainly localized at the C═O bond farthest from the isoprenoid chain and most closely corresponds to the TMQ mode calculated at 1741 cm^{-1}. The 1732 cm^{-1} PQ mode analogous to the TMQ mode at 1736 cm^{-1} is an antisymmetric C═O stretch involving both carbonyls and may be responsible for the experimentally observed shoulder on the peak assigned to PQ_9's C═O stretch.[12,13] The PQ vibration at 1709 cm^{-1} (1714 cm^{-1} for TMQ) is a combination of symmetric C═C and C═O stretching, while the 1672 cm^{-1} vibration (1673 cm^{-1} for TMQ) is exclusively an antisymmetric C═C stretch. The small differences in calculated C═O and C═C stretching frequencies for TMQ vs PQ agree with experimental data for PQ_9 and TMQ.[12,13,23] An additional mode of PQ, at 1726 cm^{-1}, contains some C═O stretching character, but is mainly an isoprenoid C═C stretching mode. Although B3LYP calculations for other *p*-benzoquinones[14] overestimate the C═O and C═C stretching frequencies, the ordering and frequency differences between modes for TMQ and PQ are qualitatively correct.

The primary difference in the calculated vibrations of the neutral molecules and their radical anions lies in the order of the C═O and C═C stretching frequencies. In the neutral molecules the CO modes are predicted at higher frequencies, while in the radical anions the C═C modes are higher. In $PQ^{\bullet-}$ a nearly pure C═C symmetric stretching vibration is calculated at 1664 cm^{-1}. Next in frequency is a combination of C═C and CO antisymmetric stretching modes at 1561 cm^{-1}. Slightly lower in frequency is another combination of C═O and C═C antisymmetric stretches at 1550 cm^{-1}. Finally, a pure CO symmetric stretching mode is calculated at 1534 cm^{-1}. The ordering of the $TMQ^{\bullet-}$ modes is similar to that described for $PQ^{\bullet-}$, although calculated frequencies (at 1668, 1562, 1542, and 1556 cm^{-1}, respectively) are each slightly higher.

Electron Affinities and Aqueous Reduction Potentials

Table 4 shows calculated electron affinities for TMQ, the model PQ, and PQ_1 as well as calculated aqueous one-electron reduction potentials for TMQ and PQ_1. The calculated electron affinity for TMQ of 1.66 eV[24] compares very well with the experimental value of 1.63 eV.[25] The calculated electron affinity for PQ is 1.80 eV, higher than our predicted electron affinity for PQ_1 of 1.75 eV. Although the difference in calculated electron affinities for PQ and PQ_1 is within the error range of the calculation (approximately 0.05 eV[24]) and no experimental

TABLE 2: Comparison of Calculated Vibrational Frequencies (in cm^{-1}) for the Plastoquinone Model (PQ) and Its Radical Anion ($PQ^{\bullet-}$)

mode	description	PQ	$PQ^{\bullet-}$
69	chain C−H str	3238	3209
68	ring C−H str	3202	3151
67	chain C−H str	3187	3183
66	methyl C−H stretch	3170	3138
65	methyl C−H stretch	3169	3137
64	chain C−H stretch	3156	3132
63	chain C−H stretch	3104	3066
62	methyl C−H stretch	3096	3039
61	methyl C−H stretch	3089	3037
60	chain C−H stretch	3048	3012
59	methyl C−H stretch	3047	3002
58	methyl C−H stretch	3044	3005
57	C_1═O_7 stretch	1738	1664
56	C═O asym. stretch	1732	1534
55	C_6═C_8/chain C═C stretch	1726	1721
54	C═O/ring C═C sym. stretch	1709	1561
53	ring C═C asym. stretch	1672	1550
52	methyl rotation	1532	1540
51	methyl rotation	1519	1528
50	C_{Me}−H bend	1511	1516
49	C_{Me}−H bend	1507	1508
48	C_{Ch}−H bend	1500	1488
47	C_{Ch}−H bend	1471	1464
46	C_{Me}−H bend	1435	1410
45	C_{Me}−H bend	1428	1400
44	ring stretch/bend	1388	1447
43	chain stretch/torsion	1346	1331
42	ring stretch/bend	1333	1343
41	chain stretch/torsion	1323	1302
40	ring/ring−methyl stretch	1290	1229
39	chain stretch/torsion	1245	1250
38	ring−chain stretch/ring bend	1207	1203
37	ring−methyl rock/ring bend	1138	1123
36	chain torsion/ring−methyl stretch	1127	1128
35	chain stretch/torsion	1117	1138
34	ring−methyl rock	1076	1077
33	chain stretch/torsion	1048	1069
32	ring−methyl rock	1039	1045
31	ring−methyl rock/ring stretch	1027	1022
30	chain stretch/torsion	967	962
29	ring−chain/ring methyl stretch	949	940
28	ring−H rock OOP	942	890
27	ring−H rock IP	931	930
26	ring−H stretch/ring stretch	904	876
25	ring−methyl rock/ring stretch	828	848
24	ring torsion (chair)	799	774
23	ring stretch/bend	749	744
22	ring torsion (boat)/stretch	695	690
21	chain torsion/ring bend	656	664
20	ring bend/chain torsion	645	644
19	ring stretch/chain torsion	556	566
18	ring torsion (boat)	520	528
17	ring stretch/chain bend	474	487
16	ring bend	455	467
15	ring/chain torsion	428	423
14	C═O bend/ring bend	422	411
13	ring bend/chain stretch	368	363
12	ring bend/ring−methyl rock	341	341
11	ring−methyl rock	303	301
10	ring−methyl rock	282	294
9	ring torsion	255	276
8	chain stretch/ring torsion (chair)	213	227
7	chain stretch/ring torsion (boat)	137	158
6	methyl rotation	120	156
5	ring torsion (chair)	114	139
4	chain stretch/ring torsion (boat)	88	113
3	methyl rotation	68	121
2	chain torsion	55	55
1	methyl rotation	48	66

TABLE 3: Comparison of Calculated Vibrational Frequencies (in cm^{-1}) for Trimethyl-*p*-Benzoquinone (TMQ) and Trimethyl-*p*-benzosemiquinone Anion ($TMQ^{\bullet-}$)

mode	description	TMQ	$TMQ^{\bullet-}$
57	ring C−H stretch	3198	3142
56	methyl C−H stretch	3167	3134
55	methyl C−H stretch	3165	3132
54	methyl C−H stretch	3143	3093
53	methyl C−H stretch	3115	3068
52	methyl C−H stretch	3096	3035
51	methyl C−H stretch	3088	3033
50	methyl C−H stretch	3058	3022
49	methyl C−H stretch	3046	2999
48	methyl C−H stretch	3043	3002
47	C═O sym. stretch	1741	1541
46	C═O asym. stretch	1736	1556
45	C═C sym. stretch	1714	1668
44	C═C asym. stretch	1673	1562
43	HCH bend	1533	1542
42	HCH bend	1519	1527
41	HCH bend	1509	1516
40	HCH bend	1507	1511
39	HCH bend	1507	1509
38	HCH bend	1499	1500
37	C_{Me}−H bend	1442	1424
36	C_{Me}−H bend	1433	1409
35	C_{Me}−H bend	1428	1398
34	ring stretch/bend	1382	1451
33	ring stretch/bend	1332	1335
32	ring stretch/bend	1284	1231
31	ring−methyl stretch	1215	1213
30	C_{Me}−H bend	1136	1123
29	ring−methyl stretch	1121	1140
28	C_{Me}−H bend	1078	1079
27	C_{Me}−H bend	1074	1067
26	C_{Me}−H bend	1056	1044
25	C_{Me}−H bend	1040	1047
24	C_{Me}−H bend	1018	1015
23	ring−methyl stretch	939	946
22	ring−H rock OOP	909	875
21	ring stretch/bend	829	853
20	ring torsion (chair)	789	759
19	ring bend	704	714
18	ring torsion (boat)	688	680
17	C═O bend	647	648
16	ring stretch/bend	563	576
15	ring torsion OOP	513	518
14	ring bend	471	487
13	C═O bend	421	401
12	ring bend	411	436
11	ring−methyl wag	372	390
10	ring−methyl rock	341	339
9	ring−methyl rock	306	307
8	ring−methyl rock	279	279
7	ring−methyl wag	259	281
6	ring torsion (chair)	173	186
5	methyl rotation	137	155
4	methyl rotation	114	139
3	ring methyl wag	113	119
2	ring torsion (boat)	75	102
1	methyl rotation	61	118

electron affinities are available for comparison, their difference implies that the isoprenoid chain's methyl groups lower the electron affinity.

Although the calculated aqueous one-electron reduction potential for PQ_1 is only 0.06 eV less than the experimental value, it is 0.11 eV higher than the reduction potential calculated for TMQ. Since the experimental reduction potentials for TMQ and PQ_1 are identical,[5] our calculations show a discrepancy between the two reduction potentials slightly larger than the error range of the calculations (0.1 eV).[26,27] The source of the difference in calculated reduction potentials for PQ_1 and TMQ is currently unknown and we are testing the influence of different conformations on electron affinities and hydration free energy differences. Finally, we note that the calculated hydration free energy difference between TMQ and $TMQ^{\bullet-}$ (2.45 eV) is almost identical to that between PQ_1 and $PQ_1^{\bullet-}$ (2.47 eV).

TABLE 4: Calculated and Experimental Electron Affinities and Reduction Potentials (eV) for Plastoquinone-1 and Trimethyl-*p*-benzoquinone

	PQ (model)	plastoquinone-1		trimethyl-*p*-benzoquinone	
	calcd	calcd	exptl	calcd	exptl
electron affinity	1.80	1.75	n/a[c]	1.66	1.63[a]
reduction potential	n/a[c]	4.22	4.28[b]	4.11	4.28[b]

[a] Fukuda, E. K.; McIver, R. T. *J. Am. Chem. Soc.* **1985**, *107*, 2291−2296. [b] Rich, P. R.; Bendall, D. S. *Biochim. Biophys. Acta* **1980**, *592*, 506−518. [c] n/a = not available.

Conclusions

Structures, spin densities, hyperfine coupling constants, and vibrational frequencies were calculated for trimethyl-*p*-benzoquinone (TMQ), a model for plastoquinone-1 without methyl groups on the isoprenoid side chain (PQ), and their radical anions by using the hybrid Hartree−Fock/density functional B3LYP/6-31G(d) method. In addition, aqueous one-electron reduction potentials were calculated for TMQ and plastoquinone-1 (PQ_1) by combining hydration free energy differences from free energy perturbation/molecular dynamics simulations with electron affinities derived by using the B3LYP method. Calculated bond distances within the quinoidal head groups of TMQ and PQ differ by less than 0.001 Å, and bond distances within the corresponding anions are comparably close. Hyperfine coupling constants and atomic spin densities calculated for the two radical anions are also nearly identical. Although calculated vibrational frequencies for TMQ and $TMQ^{\bullet-}$ are slightly higher than the corresponding frequencies for PQ and $PQ^{\bullet-}$, respectively, the important C═O and C═C stretching frequencies differ by only 1−8 cm^{-1}. Calculated hydration free energy differences between the molecules and their radical anions differ by less than 0.02 eV, whereas calculated electron affinities for TMQ and PQ_1 differ from each other by 0.09 eV. Consequently, calculated aqueous one-electron reduction potentials differ by 0.11 eV, approximately the error range of the calculations. $TMQ/TMQ^{\bullet-}$ therefore represent excellent structural and spectroscopic models for $PQ/PQ^{\bullet-}$ in isolation and very good thermochemical models in aqueous solutions. Future studies might address the adequacy of $TMQ/TMQ^{\bullet-}$ as models of $PQ/PQ^{\bullet-}$ in proteins.

Acknowledgment. The research discussed in this publication was made possible by OCAST award number HN3-011 from the Oklahoma Center for the Advancement of Science and Technology and by supercomputer time grants from the NSF/MetaCenter Allocations Committee, the NSF/National Center for Supercomputing Applications, and the NSF/Cornell Theory Center. The Cornell Theory Center receives major funding from the NSF and New York State. Additional funding comes from ARPA, the NIH, IBM Corp., and other members of the center's Corporate Research Institute. We are also grateful for supercomputer time at the University of Oklahoma made possible by support from IBM Corporation (in part through a Shared University Research grant), Silicon Graphics, Inc. and the University of Oklahoma. A.K.G. thanks the Phillips Petroleum Foundation and the University of Oklahoma Department of Chemistry & Biochemistry for fellowship support.

SCHEME 2

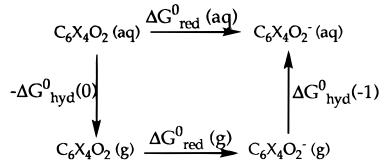

Appendix

Computational Methods. Geometry optimizations were done by using the B3LYP/6-31G(d) hybrid Hartree−Fock/density functional method,[28,29] within the GAUSSIAN94 and GAUSSIAN92/DFT computer programs. This combination of method and basis set gave bond distances within experimental error of gas-phase electron diffraction bond distances for related quinones including *p*-benzoquinone, *p*-chloroanil, and *p*-fluoranil.[14] To calculate a minimum energy orientation of the isoprenoid side chain we performed optimizations starting from six noneclipsed conformations of the chain for the neutral and anionic forms. Three energy minima for the dihedral angle about the central C−C bond of the isoprenoid chain were found at 109°, 358°, and 243°, with the latter angle having the lowest energy for PQ. Similar results were obtained for the radical anion $PQ^{\bullet-}$ whose lowest energy conformation has a dihedral angle of 237°. Spin densities were obtained by using Mulliken population analysis[31] (and the 6-311G(d,p) basis) and are therefore only qualitatively correct. Hyperfine coupling constants were obtained by using three different basis sets, including one developed by Chipman specifically for calculating hfccs using molecular orbital methods (calculated at the B3LYP/6-31G(d) geometry). The Chipman basis, denoted [632|41], is double-ζ quality, augmented by diffuse and double polarization functions as well as a tighter inner s function on hydrogen.[21,22] Vibrational frequency calculations also used the B3LYP/6-31G(d) method. Mode assignments were performed by calculating total energy distributions[32] using the GAMESS[33,34] quantum chemistry program and by animating each mode using the program XMOL.[35]

Aqueous one-electron reduction potentials were computed by using the thermodynamic cycle shown in Scheme 2. The reduction free energy is the sum of free energies for the indirect route from reactants to products, ΔG^0_{red} (aq) = ΔG^0_{red}(g) + $\{\Delta G^0_{hyd}(-1) - \Delta G^0_{hyd}(0)\}$. The free energy perturbation (FEP) method with molecular dynamics[36−44] was chosen to calculate hydration free energy differences, and the B3LYP/6-311G(d,p) method was used to calculate electron affinities as an approximation to ΔG^0_{red}(g). The B3LYP/6-311G(3d,p) method was shown to give electron affinities with an average absolute error of only 0.05 eV for a series of 14 *p*-benzoquinones, and the 6-311G(d,p) basis set is almost as good.[24] The 6-31G(d) optimized geometries were used as starting points for geometry optimizations using the larger basis set. The energy differences between the optimized neutral and anionic structures approximate adiabatic electron affinities.

The protocol for our MD simulations is described elsewhere[26,27] and will be summarized here. Simulations were performed for a constant pressure (1 atm), temperature (300 ± 20 K), and number of atoms by using the AMBER MD programs.[45] Bond distances were held constant by using the SHAKE coordinate resetting algorithm[46,47] to allow use of a 0.001 ps time step and all structures were equilibrated for at least 100 ps before beginning FEP calculations. A single molecule or ion was solvated by 647 (trimethyl-*p*-benzoquinone) or 1200 (plastoquinone) TIP3P water molecules[48] in a rectangular box incorporating periodic boundary conditions. Interactions in solution were cut off beyond 10 Å, and a Born charging correction[49−51] was applied. The dielectric constant was assumed the same as the experimental dielectric constant of water, 78.

Force fields for TMQ, $TMQ^{\bullet-}$, PQ, and $PQ^{\bullet-}$ were determined by a procedure identical to that used previously for a number of other *p*-benzoquinones.[26,27] First, Lennard-Jones parameters were adopted from those for similar atom types in the works of Weiner et al. (with a united atom model for side chains).[52,53] Partial atomic charges were determined by using the program CHELPG[54] to perform a least-squares fit to find charges that best reproduce the electrostatic potential on a grid of points (generated from our B3LYP/6-31G(d) calculations). The grid was chosen to include at least 13 000 points spaced 0.3 Å apart and located outside the van der Waals radius of each atom. Force constants were obtained by calculating unscaled B3LYP force constants for internal coordinates. For torsional angle twisting, the harmonic force constants were adapted for use in AMBER by using a trigonometric identy to relate the functional form of the AMBER torsional potential, $V_n/2[\cos(n\phi-\phi_o)]$, to sines and cosines of the individual angles $n\phi$ and ϕ_o, noting that the equilibrium torsional angle ϕ_o is 180° for each torsional angle required (except for PQ's isoprenoid chain), and expanding cos(nϕ) in a Taylor series to obtain the approximate relation $V_n/2 = K_\phi/n^2$ (where K_ϕ are unscaled harmonic force constants obtained from the B3LYP/6-31G(d) calculations). Additional tests indicate that hydration free energy differences are independent of the force constants chosen, within reasonable limits. Although FEP simulations neglect electronic polarization effects, we have tested an alternate thermodynamic cycle that transforms between species of the same total charge and found that aqueous one-electron reduction potentials for several quinones including TMQ are almost identical with those calculated by using the cycle shown in Scheme 2, within the error limits of the calculations.[27]

References and Notes

(1) Hansson, Ö.; Wydrzynski, T. *Photosynth. Res.* **1990**, *23*, 131−162 and references therein.

(2) Staehelin, L. A.; Arntzen, C. J., Eds. *Photosynthesis III: Photosynthetic Membranes and Light Harvesting Systems*; Springer-Verlag: Berlin, 1986.

(3) Trumpower, B. L., Ed. *Function of Quinones in Energy Conserving Systems*; Academic: New York, 1982.

(4) Morton, R. A., Ed. *Biochemistry of Quinones*; Academic: London, 1965.

(5) Rich, P. R.; Bendall, D. S. *Biochim. Biophys. Acta* **1980**, *592*, 506−518.

(6) Swallow, A. J. In *Functions of Quinones in Energy Conserving Systems*; Trumpo, B. L., Ed.; Academic: New York, 1982; pp 59−72.

(7) Weil, J.; Bolton, J. R.; Wertz, J. E. *Electron Paramagnetic Resonance*; Wiley-Interscience: New York, 1994.

(8) Gordy, W. *Theory and Applications of Electron Spin Resonance*; Wiley-*Interscience*: New York, 1980.

(9) Macmillan, F.; Lendzian, F.; Lubitz, W. *Magn. Reson. Chem.* **1995**, *33*, S81−S93.

(10) Robinson, H. H.; Kahn, S. D. *J. Am. Chem. Soc.* **1990**, *112*, 4728−4731.

(11) O'Malley, P. J.; Collins, S. J. *Chem. Phys. Lett.* **1996**, *259*, 296−300.

(12) Burie, J.-R.; Boussac, A.; Boullais, C.; Berger, G.; Mattioli, T.; Mioskowski, C.; Nabedryk, E.; Breton, J. *J. Phys. Chem.* **1995**, *99*, 4059−4070.

(13) Kruk, J.; Strzalka, K.; LeBlanc, R. M. *Biophys. Chem.* **1993**, *45*, 235−244.

(14) Boesch, S. E.; Wheeler, R. A. *J. Phys. Chem.* **1995**, *99*, 8125-8134.

(15) Wheeler, R. A. *J. Phys. Chem.* **1993**, *97*, 1533−1537.

(16) Grafton, A. K.; Boesch, S. E.; Wheeler, R. A. *J. Mol. Struc. (THEOCHEM)* **1997**. In press.

(17) Macmillan, F.; Lendzian, F.; Renger, G.; Lubitz, W. *Biochemistry* **1995**, *34*, 245−267.

(18) Cohen, M. J.; Chong, D. P. *Chem. Phys. Lett.* **1995**, *234*, 405−412.

(19) Barone, V. *Theor. Chim. Acta* **1995**, *91*, 113−128 and references therein.

(20) Eriksson, L. A.; Malkin, V. G.; Malkina, O. L.; Salahub, D. R. *J. Chem. Phys.* **1993**, *99*, 9756−9763.

(21) Chipman, D. *Theor. Chim. Acta* **1989**, *76*, 73−84.

(22) Basis sets were obtained from the Extensible Computational Chemistry Environment Basis Set Database, Version 1.0, as developed and distributed by the Molecular Science Computing Facility, Environmental and Molecular Sciences Laboratory, which is part of the Pacific Northwest Laboratory, P. O. Box 999, Richland, WA 99352, and funded by the U.S. Department of Energy. The Pacific Northwest Laboratory is a multiprogram laboratory operated by Battelle Memorial Institute for the U.S. Department of Energy under Contract DE-AC06-76RLO 1830. Contact David Feller, Karen Schuchardt, or Don Jones for further information.

(23) Berthomieu, C.; Nabedryk, E.; Mäntele, W.; Breton, J. *FEBS Lett.* **1990**, *269*, 363−367.

(24) Boesch, S. E.; Grafton, A. K.; Wheeler, R. A. *J. Phys. Chem.* **1996**, *100*, 10083−10087.

(25) Fukuda, E. K.; McIver, R. T. J. *J. Am. Chem. Soc.* **1985**, *107*, 2291−2296.

(26) Wheeler, R. A. *J. Am. Chem. Soc.* **1994**, *116*, 11048−11051.

(27) Raymond, K. S.; Grafton, A. K.; Wheeler, R. A. *J. Phys. Chem. B*, in press.

(28) Stephens, P. J.; Devlin, F. J.; Chablowski, C. F.; Frisch, M. J. *J. Phys. Chem.* **1994**, *98*, 11623−11627.

(29) Frisch, M. J.; Trucks, G. W.; Schlegel, H. B.; Gill, P. M. W.; Johnson, B. G.; Robb, M. A.; Cheeseman, J. R.; Keith, T. A.; Petersson, G. A.; Montgomery, J. A.; Raghavachari, K.; Al-Laham, M. A.; Zakrzewski, V. G.; Ortiz, J. V.; Foresman, J. B.; Cioslowski, J.; Stefanov, B. B.; Nanayakkara, A.; Challacombe, M.; Peng, C. Y.; Ayala, P. Y.; Chen, W.; Wong, M. W.; Andres, J. L.; Replogle, E. S.; Gomperts, R.; Martin, R. L.; Fox, D. J.; Binkley, J. S.; Defrees, D. J.; Baker, J.; Stewart, J. J. P.; Head-Gordon, M.; Gonzalez, C.; Pople, J. A. *GAUSSIAN94*, Revisions B.2, B.3, D.1, and D.2; Gaussian, Inc.: Pittsburgh, PA, 1995.

(30) Frisch, M. J.; Trucks, G. W.; Schlegel, H. B.; Gill, P. M. W.; Johnson, B. G.; Wong, M. W.; Foresman, J. B.; Robb, M. A.; Head-Gordon, M.; Replogle, E. S.; Gomperts, R.; Andres, J. L.; Raghavachari, J. S.; Binkley, J. S.; Gonzalez, C.; Martin, R. L.; Fox, D. J.; Defrees, D. J.; Baker, J.; Stewart, J. J. P.; Pople, J. A. GAUSSIAN92/DFT, Revision G.3; Gaussian, Inc.: Pittsburgh, PA, 1993.

(31) Mulliken, R. S. *J. Chem. Phys.* **1955**, *23*, 1833−1840.

(32) Pulay, P.; Torok, F. *Acta Chim. Acad. Sci. Hung.* **1965**, *47*, 273−279.

(33) Schmidt, M. W.; Baldridge, K. K.; Boatz, J. A.; Jensen, J. H.; Koseki, S.; Gordon, M. S.; Nguyen, K. A.; Windus, T. L.; Elbert, S. T. *QCPE Bull.* **1990**, *10*, 52.

(34) Dupuis, M.; Spangler, D.; Wendoloski, J. J. *National Resource for Computations in Chemistry Catalog, Program QG01*; University of California: Berkeley, 1980.

(35) Wasikowski, C.; Klemm, S. *XMOL* Version 1.3.1; Research Equipment, Inc. Minnesota Supercomputer Center, Inc.: Minneapolis, 1993.

(36) Allen, M. P.; Tildesley, D. J. *Computer Simulation of Liquids*; Clarendon Press: Oxford, 1987.

(37) McCammon, J. A.; Harvey, S. C. *Dynamics of Proteins and Nucleic Acids*; Cambridge University: Cambridge, 1987.

(38) Reynolds, C. A.; King, P. M.; Richards, W. G. *Mol. Phys.* **1992**, *76*, 251−275.

(39) Jorgensen, W. L. *Acc. Chem. Res.* **1989**, *22*, 184−189.

(40) Kollman, P. A. *Chem. Rev.* **1993**, *93*, 2395−2417.

(41) van Gunsteren, W. F.; Berendsen, H. J. C. *Angew. Chem.* **1990**, *102*, 1020−1051.

(42) Beveridge, D. L.; DiCapua, F. M. *Annu. Rev. Biophys. Biophys. Chem.* **1989**, *18*, 431−492.

(43) Straatsma, T. P.; McCammon, J. A. *Annu. Rev. Phys. Chem.* **1992**, *43*, 407−435.

(44) Warshel, A.; Chu, Z. T. In *Structure and Reactivity in Aqueous Solution: Characterization of Chemical and Biological Systems*; American Chemical *Society*: Washington, DC, 1994; Vol. 568; p 71.

(45) Pearlman, D. A.; Case, D. A.; Caldwell, J. C.; Seibel, G. L.; Singh, U. C.; Weiner, P. K.; Kollman, P. A. *AMBER 4.1*, University of San Francisco: San Francisco, 1991.

(46) van Gunsteren, W. F.; Berendsen, H. J. C. *Mol. Phys.* **1977**, *34*, 1311−1327.

(47) Ryckaert, J. P.; Ciccotti, G.; Berendsen, H. J. C. *J. Comput. Phys.* **1977**, *23*, 327−341.

(48) Jorgensen, W. L.; Chandrasekhar, J.; Madura, J. D.; Impey, R. W.; Klein, M. L. *J. Chem. Phys.* **1983**, *79*, 926−935.

(49) Born, M. *Z. Phys.* **1920**, *1*, 45−49.

(50) Rashin, A. A.; Honig, B. *J. Phys. Chem.* **1985**, *89*, 5588−5593.

(51) Jayaram, B.; Fine, F.; Sharp, K.; Honig, B. *J. Phys. Chem.* **1989**, *93*, 4320−4327.

(52) Weiner, S. J.; Kollman, P. A.; Case, D. A.; Singh, U. C.; Ghio, C.; Alagona, G.; Profeta, S.; Weiner, P. *J. Am. Chem. Soc.* **1984**, *106*, 765−784.

(53) Weiner, S. J.; Kollman, P. A.; Nguyen, D. T.; Case, D. A. *J. Comput. Chem.* **1986**, *7*, 230−252.

(54) Breneman, C. M.; Wiberg, K. B. *J. Comput. Chem.* **1990**, *11*, 361−373.